

1 **A novel functional single-cell approach to probing**
2 **nitrogen-fixing bacteria in soil communities by**
3 **resonance Raman spectroscopy with $^{15}\text{N}_2$ labelling**

4
5 *Li Cui,[†] Kai Yang,^{†,‡} Hong-Zhe Li,^{†,‡} Han Zhang,[†] Jian-Qiang Su,[†] Maria*

6 *Paraskevaidi,[§] Francis L Martin,[§] Bin Ren,^δ Yong-Guan Zhu,^{*,†,θ}*

7
8 [†]Key Lab of Urban Environment and Health, Institute of Urban Environment,
9 Chinese Academy of Sciences, Xiamen 361021, China. [‡]University of Chinese
10 Academy of Sciences, 19A Yuquan Road, Beijing 100049, China. ^θState Key
11 Laboratory of Urban and Regional Ecology, Research Center for Eco-Environmental
12 Sciences, Chinese Academy of Sciences, Beijing 100085, China. [§]School of
13 Pharmacy and Biomedical Sciences, University of Central Lancashire, Preston PR1
14 2HE, UK. ^δDepartment of Chemistry, Xiamen University, Xiamen 361005, China.

15 Li Cui and Kai Yang contributed equally to this work.

16

17

TOC/Abstract art

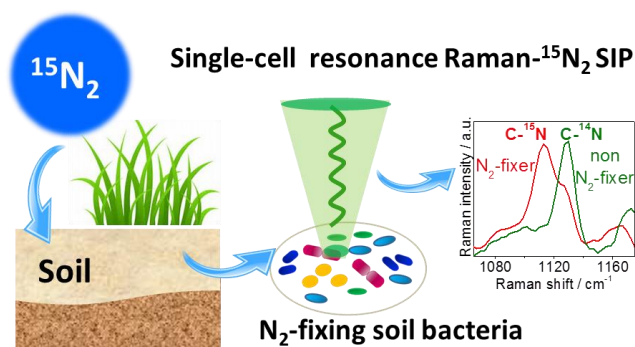
18

19

20

21

22



23 **ABSTRACT**

24 Nitrogen (N) fixation is the conversion of inert nitrogen gas (N₂) to bioavailable N
25 essential for all forms of life. N₂-fixing microorganisms (diazotrophs), which play a
26 key role in global N cycling, remain largely obscure because a large majority are
27 uncultured. Direct probing of active diazotrophs in the environment is still a major
28 challenge. Herein, a novel culture-independent single-cell approach combining
29 resonance Raman (RR) spectroscopy with ¹⁵N₂ stable isotope probing (SIP) was
30 developed to discern N₂-fixing bacteria in a complex soil community. Strong RR
31 signals of cytochrome c (Cyt c, frequently present in diverse N₂-fixing bacteria),
32 along with a marked ¹⁵N₂-induced Cyt c band shift, generated a highly
33 distinguishable biomarker for N₂ fixation. ¹⁵N₂-induced shift was consistent well with
34 ¹⁵N abundance in cell determined by isotope ratio mass spectroscopy. By applying
35 this biomarker and Raman imaging, N₂-fixing bacteria in both artificial and complex
36 soil communities were discerned and imaged at the single-cell level. The linear band
37 shift of Cyt c *versus* ¹⁵N₂ percentage allowed quantification of N₂ fixation extent of
38 diverse soil bacteria. This single-cell approach will advance the exploration of
39 hitherto uncultured diazotrophs in diverse ecosystems.

40

41 Keywords: single-cell resonance Raman, N₂-fixing bacteria, ¹⁵N₂ stable isotope
42 probe, cytochrome c, soil community

43

44

45 **INTRODUCTION**

46 Nitrogen (N) is an essential element sustaining all forms of life on Earth. Biological
47 fixation is a critical process converting inert nitrogen gas (N₂) to bioavailable N
48 (ammonia or nitrate) required by all living organisms for biosynthesis. It has been
49 estimated that over half of the fixed N sustaining the world's population is supplied
50 by biological fixation.^{1,2} This process is exclusively performed by bacteria and
51 archaea (diazotrophs) in free-living form³ or in symbiosis with coral,⁴ higher plants,⁵
52 or animals in different ecosystems.⁶⁻⁹ Despite the importance of biological N₂
53 fixation, active diazotrophs along with their distribution in ecosystems, remain
54 largely unknown.^{10,11} One important reason is that a large proportion of diazotrophs
55 remain uncultured to date.

56 Molecular methods exploiting nitrogenase *nifH* genes have been widely used to
57 evaluate the potential of N₂ fixation in diverse ecosystems in a culture-independent
58 fashion.^{9,10,12,13} Microorganisms expressing *nifH* genes, including a large portion of
59 uncultured bacteria, were reported to have the genetic potential for N₂ fixation.^{7,10,14}
60 However, discordance between presence or transcription of *nifH* and N₂-fixation
61 activity has been revealed,^{12,13} suggesting that species with genetic potential do not
62 necessarily fix N₂. Hence, a functional or phenotypic means of identification of
63 N₂-fixing microorganisms is urgently needed. Stable isotope probing (SIP) with ¹⁵N₂
64 is reported to be the only direct and unambiguous means for identifying N₂-fixing
65 bacteria and quantifying biological N₂ fixation.^{15,16} Combining ¹⁵N₂ SIP with
66 single-cell level characterization provides additional advantages of allowing one to
67 bypass the need for culture, whilst imaging of distribution of N₂-fixation species in
68 complex communities such as bacteria-protist symbionts.⁷ ¹⁵N₂-SIP combined with
69 high spatial resolution secondary ion mass spectroscopy (SIMS) - especially

70 NanoSIMS - is one of the very few available techniques that can probe active
71 N₂-fixing bacteria at the single-cell level.^{6,7,10,12,17,18} By applying single-cell
72 NanoSIMS to analyze ¹⁵N₂-incubated sample, a novel cyanobacterial group actively
73 fixing N₂ was discovered in a microbial mat; in contrast, despite expressing genetic
74 potential, a N₂-fixing deltaproteobacteria was excluded due to a lack of ¹⁵N
75 enrichment.^{10,12} NanoSIMS imaging of an *in vivo* ¹⁵N-labeled protist inhabiting
76 wood-eating roach revealed N₂ fixation in bacterial ectosymbionts of protist.⁷ These
77 applications advance the exploration of uncultured diazotrophs. Nevertheless, SIMS
78 is a destructive approach and thus does not allow important downstream genomic
79 sequencing or even cultivation of active N₂-fixing cells.

80 Raman spectroscopy is an attractive non-destructive method capable of providing
81 information about the chemical bonds of various biomolecules of bacteria and
82 discerning functional bacteria at the single-cell level.^{19,20} For some cells with
83 specific pigments such as cytochrome c (Cyt c), carotenoids or chlorophyll, strong
84 resonance Raman (RR) signals can be excited if the laser wavelength is within - or
85 close to - the electronic transition of molecules.²¹⁻²⁷ Selective enhancement of RR
86 generates a highly characteristic Raman feature of pigment-containing bacteria.
87 Measurement time can also be greatly reduced, facilitating a relatively rapid spectral
88 acquisition such as Raman imaging. Raman imaging is similar to NanoSIMS
89 imaging by providing information regarding the spatial distribution of bacteria in
90 microbial communities.^{21,23} More importantly, in combination with ¹³C or D₂O-SIP,
91 single-cell Raman or RR can detect functional or active cells in their natural habitat,
92 based on the Raman shift induced by substitution of 'light' atom in a chemical bond
93 by its 'heavier' isotope.^{19,28,29} Despite these advantages, ¹⁵N-induced shifts are far
94 less distinguishable than ¹³C or ²D-induced, and the few reports of single-cell Raman

95 with ^{15}N -SIP were all limited to pure-cultured bacteria.^{19,30} Recently, owing to the
96 finding of clear ^{15}N -induced shifts in surface-enhanced Raman spectra (SERS) of
97 bacteria,^{19,31} SERS was successfully applied for bulk analysis of N assimilation by
98 environmental bacterial community in a wetland.³¹ However, because SERS
99 substrates can easily be contaminated by environmental medium and damaged by
100 laser, single-cell SERS has not been achieved in complex environmental microbial
101 communities. In this regard, normal Raman or RR spectroscopy is more feasible
102 towards investigating environmental bacteria. To date, there is no report using
103 single-cell Raman to study N_2 -fixing bacteria in complex ecosystems. Identifying an
104 indicative Raman band associated with N_2 fixation is the priority for the potential
105 applicability of this approach.

106 Herein, we showed for the first time that $^{15}\text{N}_2$ -induced shifts in the resonance
107 Raman band of Cyt c are a sensitive and robust indicator of N_2 -fixation. This
108 biomarker was then used to discern and image the location of N_2 -fixing bacteria in
109 both artificial and complex soil communities at the single-cell level. The linear band
110 shift *versus* $^{15}\text{N}_2$ percentages provided a good means to compare N_2 fixation extent
111 of diverse soil bacteria. This work provides a novel single-cell resonance Raman
112 approach to discern, image and compare fixation extent of N_2 -fixing soil bacteria.

113

114 **MATERIALS AND METHODS**

115 **Strains, media and growth conditions.** Four model N_2 -fixing bacteria, including
116 two free-living *Azotobacter* sp. (AS1.222) and *Azotobacter chroococcum*
117 (ACCC10096), two symbiotic *Rhizobium radiobacter* (ATCC15955) and
118 *Bradyrhizobium japonicum* (ACCC15067), were purchased from Guangdong
119 Culture Collection Center of Microbiology, China. *Azotobacter* sp. and A.

120 *chroococcum* were cultured in N-free azotobacter media containing 20 g L⁻¹
121 mannitol, 0.2 g L⁻¹ KH₂PO₄, 0.8 g L⁻¹ K₂HPO₄, 0.2 g L⁻¹ MgSO₄ · 7H₂O, 0.1 g L⁻¹
122 CaSO₄ · 2H₂O, and trace amount of Na₂MoO₄ · 2H₂O and FeCl₃ at 28 °C and 180 rpm.
123 *R. radiobacter* and non-N₂-fixing strain *Shewanella oneidensis* MR-1 were grown in
124 Luria Bertani (LB) broth containing 10 g L⁻¹ tryptone (Oxoid Ltd., England), 5 g L⁻¹
125 yeast extract (Oxoid Ltd., England), and 10 g L⁻¹ NaCl at 28 °C and 180 rpm. *B.*
126 *japonicum* were grown in media containing 1 g L⁻¹ yeast exact, 200 mL of soil
127 extract and 10 g L⁻¹ mannitol at 28 °C and 180 rpm. Unless otherwise stated,
128 chemicals were purchased from Sinopharm Chemical Reagent Co., China.

129 **Soil sample collection.** Park soil samples were collected from grassland at a depth <
130 5 cm in the campus of Institute of Urban Environment, Xiamen, China
131 (24°36'39.90"N 118°03'33.48"E). The soil samples were homogenized and sieved
132 through a 0.6-mm sieve to remove small stones, grass roots and other debris, then
133 stored at 4 °C prior to use.

134 **Incubation of model N₂-fixing bacteria and soil microcosm with ¹⁵N₂ gas.** An
135 aliquot of 20 mL N-free azotobacter media was filled into a 40-mL crimp-top vial
136 and then inoculated with 20 µL of *Azotobacter* sp. or *A. chroococcum* after 24-hour
137 culture. Vials were sealed, and air in the headspace was replaced with mixture gas
138 consisting of ¹⁵N₂ (99 atom%, purity >98.5%, Aladdin, China) and oxygen (volume
139 ratio of N₂ to O₂ is 4:1) of different volumes to achieve ¹⁵N₂ of different percentages
140 (¹⁵N₂/(¹⁵N₂+¹⁴N₂)). Considering that ¹⁵N content is 99% in commercial ¹⁵N₂ and 0.36%
141 in natural abundance,³² the final ¹⁵N abundance relative to N₂ in air in the headspace
142 was 99.36%, 49.68%, 25.02%, 10.22%, 0.36%, respectively. Bacteria incubated with
143 different percentages of ¹⁵N₂ were harvested after culturing for 48 h. Soil microcosm
144 contained 2 g of park soil in a 12 mL crimp-top vial. Vials were sealed, purged with

145 O₂ for 10 min to remove air and then replaced with appropriate volume of ¹⁵N₂ to
146 achieve 80% ¹⁵N₂ and 20% oxygen in the headspace. The control soil microcosm
147 was supplied with lab air. ¹⁵N₂-incubated soil microcosm and control were amended
148 with 500 uL of 0.5 M glucose solution and incubated at room temperature (ca. 25 °C)
149 under low light conditions for 12 days. All of these incubations were performed in
150 triplicate.

151 **Extracting bacteria from soil microcosms by Nycodenz density gradient**
152 **separation.** Nycodenz density gradient separation was used to extract bacteria from
153 soil. A modified protocol from a previous report was used.¹⁷ Briefly, soils
154 post-incubation were homogenized in 10 mL PBS (NaCl 8 g L⁻¹, KCl 0.2 g L⁻¹,
155 Na₂HPO₄ 1.44 g L⁻¹, KH₂PO₄ 0.24 g L⁻¹) supplemented with 0.5% (v/v) Tween 20
156 (Aladdin) to detach soil particle-associated cells by vigorously vortexing for 30 min
157 at room temperature. To separate bacteria from soil particles, 1 vol of the
158 as-prepared soil slurries were introduced into an Eppendorf tube containing 1 vol of
159 Nycodenz (≥98%, Aladdin) stock solution carefully. Nycodenz stock was prepared
160 by dissolving 8 g of Nycodenz in 10 mL sterile water, producing a final density of
161 1.42 g·mL⁻¹. This density is proper for efficient capture of soil bacteria and
162 separation from soil particles.^{17,33} The tube was then centrifuged at 14000 g for 90
163 min at 4 °C. The upper and middle aqueous layers containing bacteria were collected
164 and mixed with 10 vol PBS in a fresh centrifuge tube. The bacteria inside were then
165 collected by centrifuging at 5000 rpm for 10 min and washed with ultrapure water
166 twice for further Raman analysis.

167 **Single-cell Raman measurement and Raman mapping acquisition.** To prepare
168 bacteria for single-cell Raman measurements, bacterial solution from model strains
169 or soil samples were washed twice by DI water by centrifuging at 5000 rpm for 3

170 min and then adjusting to a proper concentration in order to obtain single-cell
171 dispersion on aluminum (Al) foil substrate.³⁴ An aliquot of 2 μ L of the as-prepared
172 bacteria were loaded on Al foil and air-dried at room temperature. To construct an
173 artificial community consisting of *Azotobacter* sp. and *S. oneidensis*, one bacterial
174 solution was applied to the Al foil and allowed to air-dry whereupon the second was
175 applied to the same spot and also allowed to dry. Single-cell Raman spectra and
176 Raman mapping were obtained using a LabRAM Aramis (HORIBA Jobin-Yvon)
177 confocal micro-Raman system equipped with a 600 g/mm grating. Excitation was
178 provided by a 532-nm Nd: YAG laser. A 100 \times dry objective with a numerical
179 aperture of 0.9 (Olympus) was employed. For single-cell Raman measurements,
180 acquisition time was 5 s and 25 spectra were acquired from each bacterial sample.
181 Raman mapping was employed to generate Raman images of artificial communities
182 and also soil bacterial community containing N₂-fixing bacteria. The step-size was
183 set at 1.5 μ m in a rectangular mapping area with acquisition time of 2 s on each
184 point.

185 **Raman spectral and mapping data analysis.** LabSpec5 software (HORIBA
186 Jobin-Yvon) was used to process single-cell Raman spectra. After spectral extraction
187 and baseline subtraction (polynomial, degree 6), mean spectra from each sample
188 were calculated. The overlapped 1114 (C-¹⁵N) and 1129 cm⁻¹ (C-¹⁴N) bands were
189 deconvoluted using the GaussLorenz peak fitting function and the resulting peak
190 area was used to calculate the intensity ratio of these two bands. Principal
191 component analysis (PCA) and the required spectral pre-processing were performed
192 using IRootLab toolbox (<https://code.google.com/p/irootlab/>) running on MATLAB
193 2012a.^{35,36} Spectral pre-processing included spectral extraction (from 1095 to 1145
194 cm⁻¹), rubberband subtraction and vector normalization. PCA was then performed by

195 reducing spectral variables to 10 factors accounting for more than 99% of the total
196 variance. The resulting PCA 1-D (PC1) scores were plotted against $^{15}\text{N}_2$ percentages.
197 OriginPro8.5 was used to perform statistical calculation of average value \pm standard
198 deviation and linear regression fitting. One-way ANOVA with Tukey's Multiple
199 comparison test was conducted in GraphPad Prism 5 for significance analysis of
200 ^{15}N -induced Raman band change; $P < 0.05$ was considered significant. Direct
201 classical least square (DCLS) modelling in Labspec 5 was employed to construct a
202 Raman image of N_2 -fixing and non- N_2 -fixing bacteria based on multidimensional
203 Raman mapping data matrix. $\text{C-}^{15}\text{N}$ band at 1114 cm^{-1} and $\text{C-}^{14}\text{N}$ at 1129 cm^{-1} were
204 selected as the model, and then DCLS operation finding the linear combination of
205 model spectra that matched most closely the original data was applied to all traces of
206 the original data sets to construct Raman image of each component.

207 **Quantification of ^{15}N incorporation in N_2 -fixing bacteria by isotope ratio mass**
208 **spectroscopy (IRMS).** To measure the bulk isotope composition (^{15}N %) of
209 N_2 -fixing bacteria incubated with different percentages of $^{15}\text{N}_2$ to natural N_2 in air,
210 0.01-0.05 mg (dry weight) of ^{15}N -labeled lyophilized bacteria and 0.15-0.18 mg of
211 urea was placed in a tin capsule. For non labeled N_2 -fixing bacteria, 1 mg of
212 lyophilized cell powder was put in a tin capsule. Urea of 0.30-0.34 mg was used as
213 standard. Samples were analyzed with an elemental analyzer (Flash HT 2000
214 Thermo Fisher) coupled via a ConFlo IV device to the IRMS (Delta V advantage).
215 Isotope composition was calculated using the equation below:

216
$$\text{At}^{15}\text{N}\% = (\text{M}_{\text{urea}} \times 46.67\% \times 0.367\% + \text{M}_{\text{bacteria}} \times 9.77\% \times ^{15}\text{N}\%) / (\text{M}_{\text{urea}} \times 46.67\% + \text{M}_{\text{bacteria}} \times$$

217 $9.77\%),$ where $\text{At}^{15}\text{N}\%$ is the percentage of ^{15}N in total N and can be measured by
218 IRMS, M_{urea} and $\text{M}_{\text{bacteria}}$ are the weight of urea and bacteria in tin capsule, 0.367% is
219 the natural abundance of ^{15}N in urea, 46.67% and 9.77% are the total nitrogen

220 content in urea and bacteria respectively, $^{15}\text{N}\%$ is the abundance of ^{15}N in bacteria
221 that will be calculated.

222 **RESULTS AND DISCUSSION**

223 **Resonance Raman spectra of cytochrome c is a common signal in diverse** 224 **N_2 -fixing bacteria.**

225 To identify a common Raman signal in diverse N_2 -fixing bacteria, we examined
226 four model N_2 -fixing bacteria including two rhizobium-originated (*B. Japonicum*
227 and *R. radiobacter*) and two free-living (*Azotobacter* sp. and *A. chroococcum*), and
228 five environmental N_2 fixers isolated from soil by plating soil slurry onto N-free agar
229 plates. Only N_2 -fixing bacteria can form colonies on these agar plates since
230 atmospheric N_2 provided the sole nitrogen source required for their growth. These
231 soil N_2 -fixing isolates were affiliated to the genera of *Azotobacter*, *Rhizobium* and
232 *Raoultella* based on 16S rRNA sequencing and phylogenetic analysis (Figure S1a).
233 These genera were reported to be from N_2 -fixer group.^{9,37} To further confirm N_2
234 fixation potential of these strains, Dinitrogenase reductase genes (*nifH*), which are
235 the most widely used marker gene to identity N_2 -fixing bacteria, were amplified and
236 visualized on agarose gel. All the model and soil N_2 -fixer isolates displayed a band
237 specific to *nifH* genes, which, however, are absent in non N_2 -fixing *S. oneidensis*,
238 *E.coli* and non-templated control (Figure 1a). Phylogenetic analysis of *nifH*
239 amplicons further supported that these five soil isolates were N_2 fixers (Figure S1b).

240 Single-cell Raman spectra were acquired from four model N_2 -fixing bacteria and
241 all colonies (approximately 32) formed by N_2 -fixing soil bacteria (Figure 1b). It is
242 interesting to find that all of them display characteristic Raman bands of Cyt c at 749
243 cm^{-1} (pyrrole breathing mode), 1129 [$\nu(\text{C-N})$], 1312 [$\delta(\text{C-H})$], and 1589 cm^{-1}
244 [$\nu(\text{C-C})$], which are almost the same as that of pure Cyt c.^{21,38,39} Strong Cyt c signal

245 was also recently reported in symbiotic rhizobia isolated from legumes nodules.⁴⁰
246 These observations demonstrate that Cyt c is commonly present in both free-living
247 and symbiotic N₂-fixing bacteria of either model or environmental strains. The
248 existence of Cyt c in diazotrophs is associated with the crucial role of Cyt c in
249 protecting respiration as a terminal oxidase by rapid consumption of O₂ affecting the
250 activity of O₂-labile nitrogenase.⁴¹ In addition, intensities of Cyt c relative to Amide
251 I at 1664 cm⁻¹ were found to fluctuate in these N₂-fixer. Both the physiological state
252 of bacteria and the redox state of Cyt c were reported to affect Cyt c intensity. For
253 instance, significantly higher Cyt c signal was observed in *Rhizobium*
254 *leguminosarum* bv. *viciae* isolated from nodules than those grown in culture;⁴⁰
255 reduced state of Cyt c generated more intense signal than the oxidized state due to
256 shift in electronic transition.²³ In addition, Raman signal of Cyt c is much stronger
257 than that of other intracellular bacterial constituents, such as bands at 1002 cm⁻¹
258 (phenylalanine), 1240 cm⁻¹ (protein), 1450 cm⁻¹ (lipid) and 1664 cm⁻¹ (protein),
259 despite their higher abundance. Cyt c is a heme protein showing maximum electronic
260 absorption at around 550 nm,⁴² matching well with the 532 nm laser and thus
261 generating a selective resonance Raman enhancement.

262 Not only N₂-fixing bacteria show Cyt c RR peaks, RR signals of Cyt c have also
263 been reported in nitrifier bacteria, anaerobic bacteria, and electron-generating
264 bacteria such as *S. oneidensis* (Figure 1b) and *Geobacter*.^{21,23} Therefore, despite the
265 fact that the strong and characteristic Raman signal of Cyt c makes it highly
266 distinguishable, it is insufficient to identify N₂-fixing bacteria because Cyt c is also
267 present in other bacteria that are unable to fix nitrogen. Among the four RR bands of
268 Cyt c, the band at 1129 cm⁻¹ was assigned to C-N stretch, providing a good potential

269 target to incorporate $^{15}\text{N}_2$ stable isotope into C-N. The resulting Raman shift would
270 then provide additional evidence for N_2 fixation.

271

272 **$^{15}\text{N}_2$ -induced Raman shifts in cytochrome c are a biomarker of N_2 -fixing**
273 **bacteria**

274 To test this hypothesis, we incubated *Azotobacter* sp. and *A. chroococcum* in
275 N-free medium with different percentages of $^{15}\text{N}_2$ relative to N_2 in air, *i.e.*, 99.36%,
276 49.68%, 25.02%, 10.22% and 0.36% (^{15}N natural abundance). Mean single-cell
277 Raman spectra from approximately 25 individual cells under each $^{15}\text{N}_2$ incubation
278 conditions are shown in Figure 2a and 2b. It is notable to observe that the 1129 cm^{-1}
279 band (C-N stretch) at 0.36% $^{15}\text{N}_2$ shifted markedly to 1114 cm^{-1} at 99.36% $^{15}\text{N}_2$. The
280 around 15 cm^{-1} shift is very close to that the 13 cm^{-1} shift observed in ^{15}N
281 isotopically labeled pure Cyt c,⁴³ confirming that it is the substitution of light ^{14}N
282 with heavier ^{15}N in the C-N bond resulting in a decrease of vibrational frequency of
283 C-N stretch. By comparison, no obvious shifts were observed in other Cyt c bands
284 wherein N was absent: 749 cm^{-1} (ring breathing), 1312 cm^{-1} (C-H), 1589 cm^{-1} (C-C),
285 or bacterial composition-related bands. Figure 2b shows the enlarged spectra
286 including exclusively 1114 and 1129 cm^{-1} bands. With increasing $^{15}\text{N}_2$, the 1129
287 cm^{-1} band (C- ^{14}N) decreased whilst the 1114 cm^{-1} band (C- ^{15}N) increased. The
288 co-existence of 1129 cm^{-1} and 1114 cm^{-1} in individual bacteria indicates that only a
289 proportion of N in intracellular Cyt c is replaced by the heavier ^{15}N .

290 By deconvoluting these two bands using peak fitting in Labspec software (Figure
291 S2), peak area ratio of 1114 cm^{-1} band against the sum of peak area of 1114 cm^{-1} and
292 1129 cm^{-1} bands ($\text{Area}_{1114}/(\text{Area}_{1114}+\text{Area}_{1129})$) from individual spectrum were
293 plotted against $^{15}\text{N}_2$ percentages. A linear relationship with R^2 of 0.968 was obtained.

294 To achieve a rapid analysis of large numbers of spectra from single cells and avoid
295 possible errors in deconvolution of overlapped spectra, PCA was also performed on
296 spectral profile between 1095 and 1145 cm^{-1} (Figure 2c). Scores along PC1,
297 accounting for 87.5% of variance, generated an even better linear relationship with
298 $^{15}\text{N}_2$ percentages ($R^2 = 0.998$) than the peak area ratio ($R^2 = 0.968$).

299 To validate Raman results of N_2 fixation, bulk isotope analysis by isotope ratio
300 mass spectroscopy was used to quantify how much N was fixed in bacteria. The
301 abundance of ^{15}N in bacteria was determined to be 0.36% (close to natural
302 abundance of ^{15}N), 5.89%, 15.01%, 29.97%, and 66.16%, and linearly increased
303 with percentage of atmospheric incubation $^{15}\text{N}_2$ (Figure 2d), whereas non- N_2 fixer *S.*
304 *oneidenis* containing Cyt c and *E. coli* only displayed ^{15}N of natural abundance. This
305 measurement fully demonstrated that bacteria had incorporated ^{15}N and a higher $^{15}\text{N}_2$
306 percentage resulted in a higher incorporation extent and Raman shift. A further
307 correlation analysis indicated that ^{15}N content of bacteria corresponded linearly to
308 PC1 scores (Figure 2e), providing a way to measure the extent of N_2 fixation by RR
309 spectral profile of Cyt c at single-cell level, protist.^{16,44,45} ^{15}N abundance in bacteria
310 was around three-fifth of the $^{15}\text{N}_2$ percentage, indicating that N_2 fixers were not fully
311 labeled by ^{15}N , consistent with Raman result that both 1114 and 1129 cm^{-1} bands
312 were observed. Detection limit of Raman- $^{15}\text{N}_2$ SIP was defined as the minimum $^{15}\text{N}_2$
313 that can induce significant spectral change. Spectral change was analyzed by PCA
314 and the resulting PC1 scores were used for significance analysis of ^{15}N -induced
315 spectral change via one-way ANOVA. Detection limit was determined to be 10.22%
316 $^{15}\text{N}_2$, corresponding to 5.89% ^{15}N abundance in bacteria, at which spectra were
317 significantly different from that in air (one-way ANOVA, $P < 0.05$). The linear band
318 shifts were also obtained in *A. chroococcum* (Figure S3) with similar slope and

319 intercept ($y = 0.098x - 0.5059$) to that of *Azotobacter* sp. ($y = 0.091x - 0.5411$) based
320 on PC1 scores.

321 Bacteria without Cyt c like *E. coli* display peaks at around 1123 cm^{-1}
322 (carbohydrate), which is close to $\text{C-}^{14}\text{N}$ and $\text{C-}^{15}\text{N}$ at 1129 and 1114 cm^{-1} (Figure S4),
323 but much lower, thus will not interfere ^{15}N -induced shift. Bacteria containing
324 carotenoid show strong RR signal at 1155 and 1511 cm^{-1} . Although the band at 1155
325 cm^{-1} has some overlap with $\text{C-}^{14}\text{N}$ band of Cyt c at 1129 cm^{-1} , it separates well with
326 $\text{C-}^{15}\text{N}$ band at 1114 cm^{-1} , thus exerting no effect on identification of $^{15}\text{N}_2$ fixation.
327 Cyanobacteria can also fix N_2 ,¹² however, its fluorescence was too strong to observe
328 Raman signal (Figure S5), so RR combined with $^{15}\text{N}_2$ is not enough to detect
329 cyanobacteria as N_2 fixers. The further application of SERS with $^{15}\text{N}_2$ excited with a
330 laser out of fluorescence can provide a solution.

331 The above observations indicate that the marked $^{15}\text{N}_2$ -induced shift in C-N bond
332 of Cyt c is a sensitive and highly distinguishable biomarker for N_2 -fixing bacteria.
333 The linear shift also provides a good means towards evaluating N_2 -fixing extent in a
334 quantitative manner.

335

336 **Probing and Raman imaging of N_2 -fixing bacteria in artificial communities**

337 Important advantages of single-cell measurements lie in the ability to discern and
338 image N_2 -fixing bacteria in a complex community. Herein, an artificial community
339 comprising *S. oneidensis* and $^{15}\text{N}_2$ -incubated *Azotobacter* sp. was constructed. Both
340 species contain Cyt c, while only *Azotobacter* sp. can fix nitrogen. Raman imaging
341 was used to discern and locate $^{15}\text{N}_2$ -fixing *Azotobacter* sp. in this artificial
342 community.

343 Figure 3a shows a photomicrograph of such an artificial community with
344 *Azotobacter* sp. appearing as spherical and *S. oneidensis* as rod-shaped. Because of
345 their highly distinguishable shapes, the distribution of the two species is visually
346 relatively clear except when clumped on top of each other. By using the 1114 cm⁻¹
347 and 1129 cm⁻¹ bands characteristic of ¹⁵N-labeled N₂-fixing *Azotobacter* sp. and *S.*
348 *oneidensis* (¹⁴N) respectively (Figure 3c), Raman imaging was acquired and
349 pseudo-color Raman image was generated (Figure 3b). Red regions were identified
350 as *Azotobacter* sp. whilst green regions as *S. oneidensis*. The distribution of both
351 bacterial species in Raman images is consistent with the conventional
352 photomicrographs. For example, the encircled spherical *Azotobacter* sp. in the
353 photomicrograph can be found in the same place as that shown in red in the
354 corresponding Raman image, as is the case for *S. oneidensis*. This result
355 demonstrates the accuracy of Raman imaging in indicating the site of N₂-fixing
356 bacteria. In addition, *Azotobacter* sp. that were clumped with *S. oneidensis* (labeled
357 with arrows) were hard to confirm their presence based on the photomicrographic
358 image (Figure 3a), but can be conclusively identified to be *Azotobacter* sp. based on
359 the red spot in the Raman image, demonstrating the potential of Raman imaging in
360 locating N₂-fixing cells in microbial communities.

361

362 **Probing and Raman imaging N₂-fixing bacteria of different activities in soil** 363 **communities**

364 We further applied ¹⁵N₂ incubation and Raman imaging to reveal N₂-fixing
365 bacteria in soil microbial communities. Soils harbor a multitude of our Earth's
366 biodiversity and also a high diversity of N₂-fixing bacteria in either free form or in
367 symbiosis with plants,⁴⁶ representing the main site wherein biological N₂ fixation is

368 naturally carried out. Herein, park soil was collected from a grassland that had been
369 left fallow for a long period of time without application of fertilizer, providing a high
370 probability of detecting N₂-fixing bacteria. Soil was placed in 12-ml vials filled with
371 a mixture gas of ¹⁵N₂ (¹⁵N 99.36%) and O₂ at volume ratio of 4:1. After a 12-day
372 incubation, the soil samples were collected. To date, application of Raman
373 spectroscopy for single-cell investigations in soil systems has been very limited,¹⁷
374 because soil microorganisms are dispersed in a high background of soil particles.
375 Separation of bacteria from soil particles is a necessity for either Raman or SIMS
376 measurement.¹⁷ Soil bacteria were detached from soil particles *via* gradient density
377 centrifugation reported previously.¹⁷ High-background soil particles can be largely
378 reduced for both Raman and SIMS measurement. Figure 4 shows representative
379 Raman spectra of individual soil bacteria with different phenotypes, including
380 N₂-fixing bacteria identified by 1114 cm⁻¹ (C-¹⁵N) band (i), bacteria containing Cyt c
381 but unable to fix N₂ (ii), bacteria containing Cyt c and carotenoid of different
382 contents but unable to fix N₂ (iii, iv), as well as bacteria without any pigments (v).
383 The above finding indicates a high diversity of bacteria with different phenotypes in
384 soil.

385 Raman imaging was then applied to soil bacteria to discern and image N₂-fixing
386 bacteria. Seven areas ranging from 20×20 to 30×30 μm² were mapped. Because of
387 the high diversity of soil bacteria, not every area contained both N₂-fixer and non-N₂
388 fixer. Two areas containing both were shown in Figure 5. The photomicrograph
389 (Figure 5a, 5b left) shows soil bacteria of different shapes and sizes, but provides no
390 information on function. In contrast, we can use spectral profile covering 1114 cm⁻¹
391 and 1129 cm⁻¹ band (Figure 5c red and green) to discriminate N₂-fixing bacteria
392 from non-N₂-fixing bacteria. The resulting Raman images clearly reveal that the red

393 dots are N₂-fixing bacteria (labelled as ¹⁵N), and the green dots are non-N₂-fixing
394 bacteria containing Cyt c (Figure 5a, 5b right). Encircled bacteria (labeled with ‘no
395 Cyt c’ in Figure 5a) do not exhibit any pigment signal (Figure 5c, bottom curve
396 labeled with ‘no Cyt c’) and thus appear as a dark point in the Raman image. Figure
397 5b shows photomicrographic and Raman images taken from another independent
398 location. A total of six N₂-fixing bacteria were discerned in the two areas, including
399 two (labelled as ¹⁵N-2 and ¹⁵N-3) in close contact with non-N₂-fixing bacteria. The
400 green irregular shape connected with the ¹⁵N-2 red dot shows good consistency with
401 the photomicrographic image, indicating a sufficient spatial resolution in Raman
402 images. These observations demonstrate that Raman images can discern N₂-fixing
403 bacteria from soil communities based on their isotopic composition.

404 ¹⁵N₂-fixation extent by soil bacteria was also revealed based on spectral profile of
405 C-¹⁵N and C-¹⁴N bands. Single-cell Raman spectra from a total of 29 individual
406 N₂-fixing soil bacteria including the six identified above were incorporated together
407 with the spectra of *Azotobacter* sp. incubated with different percentages of ¹⁵N₂
408 (Figure 2c). As a comparison, three Raman spectra from soil bacteria similar to
409 *Azotobacter* sp. incubated with 0.36% ¹⁵N₂ were also incorporated; this clearly
410 indicates the presence of non- or weak N₂-fixing bacteria in soil. PCA was then
411 performed on spectra of N₂-fixer and non or weak N₂-fixer from soil to generate 1-D
412 PCA scores (on the right of Figure 2c labeled as ‘soil bacteria’). A larger variation in
413 PC1 scores was observed in soil bacteria than *Azotobacter* sp. incubated with the
414 same 99.36% ¹⁵N₂, indicating heterogeneous N₂-fixing extent from diverse soil
415 bacteria. Based on the linear correlation between ¹⁵N content measured by IRMS and
416 PC1 scores of *Azotobacter* sp. incubated with different atmospheric ¹⁵N₂% (Figure
417 2e), ¹⁵N content of soil bacteria were determined to be from 0 to 84.40 (on the right

418 of Figure 2e) by inputting PC1 scores of soil bacteria to the linear fitting equation of
419 $^{15}\text{N}\%$ in cells = $38.79 + 75.18 \times \text{PC1}$. The even larger ^{15}N incorporation extent in
420 most N_2 -fixing soil bacteria than *Azotobacter* sp. should be related to the much
421 longer incubation time of soil with $^{15}\text{N}_2$ (12 days) than *Azotobacter* sp. (2 days).

422 CONCLUSIONS

423 This is the first demonstration that single-cell resonance Raman spectroscopy with
424 $^{15}\text{N}_2$ -SIP can discern, image and compare the extent of N_2 -fixation of diverse
425 N_2 -fixing bacteria in complex soil communities in a culture-independent fashion.
426 Cyt c was demonstrated as a universal N_2 -fixation biomarker by investigating both
427 model and environmental strains screened from soils. Its strong resonance Raman
428 signal, together with a remarkable ^{15}N -induced C-N band shifts of Cyt c, provided a
429 robust biomarker to distinguish N_2 -fixing bacteria from non- N_2 -fixing bacteria with
430 or without Cyt c. Raman imaging at micrometer resolution facilitated the location of
431 N_2 -fixing bacteria in both artificial and soil communities. The linear correlation of
432 C-N band profile with $^{15}\text{N}_2$ percentages allowed a quantitative evaluation of N_2
433 fixation extent of diverse soil bacteria.

434 For future work, this single-cell resonance Raman- $^{15}\text{N}_2$ SIP approach can be
435 applied to important N_2 -fixing symbiont systems. The further combination with
436 single-cell isolation and genome sequencing suitable for soil microorganisms will
437 also be developed, in order to reveal the precise ecological role of largely
438 unexplored uncultured diazotrophs (microbial dark matter) in diverse ecosystems.

439

440 References:

441 (1) Hoffman, B. M.; Lukoyanov, D.; Yang, Z. Y.; Dean, D. R.; Seefeldt, L. C. *Chem Rev* **2014**, *114*,
442 4041-4062.

- 443 (2) Cui, S. H.; Shi, Y. L.; Groffman, P. M.; Schlesinger, W. H.; Zhu, Y. G. *Proc. Natl. Acad. Sci. U. S. A.* **2013**,
444 *110*, 2052-2057.
- 445 (3) Zehr, J. P.; Carpenter, E. J.; Villareal, T. A. *Trends Microbiol.* **2000**, *8*, 68-73.
- 446 (4) Shashar, N.; Cohen, Y.; Loya, Y.; Sar, N. *Mar Ecol Prog Ser* **1994**, *111*, 259-264.
- 447 (5) Rai, A. N.; Soderback, E.; Bergman, B. *New Phytol.* **2000**, *147*, 449-481.
- 448 (6) Lechene, C. P.; Luyten, Y.; McMahon, G.; Distel, D. L. *Science* **2007**, *317*, 1563-1566.
- 449 (7) Tai, V.; Carpenter, K. J.; Weber, P. K.; Nalepa, C. A.; Perlman, S. J.; Keeling, P. J. *Appl. Environ.*
450 *Microbiol.* **2016**, *82*, 4682-4695.
- 451 (8) Ohkuma, M.; Noda, S.; Hattori, S.; Iida, T.; Yuki, M.; Starns, D.; Inoue, J.; Darby, A. C.; Hongoh, Y.
452 *Proc. Natl. Acad. Sci. U. S. A.* **2015**, *112*, 10224-10230.
- 453 (9) König, S.; Gros, O.; Heiden, S. E.; Hinzke, T.; Thurmer, A.; Poehlein, A.; Meyer, S.; Vatin, M.;
454 Mbeguie-A-Mbeguie, D.; Toczy, J.; Ponnudurai, R.; Daniel, R.; Becher, D.; Schweder, T.; Markert, S. *Nat*
455 *Microbiol* **2016**, *2*, 16193.
- 456 (10) Woebken, D.; Burow, L. C.; Prufert-Bebout, L.; Bebout, B. M.; Hoehler, T. M.; Pett-Ridge, J.;
457 Spormann, A. M.; Weber, P. K.; Singer, S. W. *ISME J.* **2012**, *6*, 1427-1439.
- 458 (11) Sohm, J. A.; Webb, E. A.; Capone, D. G. *Nat. Rev. Microbiol.* **2011**, *9*, 499-508.
- 459 (12) Woebken, D.; Burow, L. C.; Behnam, F.; Mayali, X.; Schintlmeister, A.; Fleming, E. D.;
460 Prufert-Bebout, L.; Singer, S. W.; Corte's, A. L. p.; Hoehler, T. M.; Pett-Ridge, J.; Spormann, A. M.;
461 Wagner, M.; Weber, P. K.; Bebout, B. M. *ISME J.* **2015**, *9*, 485-496.
- 462 (13) Severin, I.; Stal, L. J. *FEMS Microbiol Ecol* **2010**, *73*, 55-67.
- 463 (14) Soares, R. A.; Roesch, L. F. W.; Zanatta, G.; Camargo, F. A. D.; Passaglia, L. M. P. *Appl Soil Ecol* **2006**,
464 *33*, 221-234.
- 465 (15) Chalk, P. M.; He, J.-Z.; Peoples, M. B.; Chen, D. *Soil Biol. Biochem.* **2017**, *106*, 36-50.
- 466 (16) Roey Angel; Christopher Panhölzl; Raphael Gabriel; Craig Herbold; Wolfgang Wanek; Andreas
467 Richter; Stephanie A. Eichorst; Woebken, D. *Environ. Microbiol.* **2018**, *20*, 44-61.
- 468 (17) Eichorst, S. A.; Strasser, F.; Woyke, T.; Schintlmeister, A.; Wagner, M.; Woebken, D. *FEMS Microbiol.*
469 *Ecol.* **2015**, *91*, fiv106.
- 470 (18) Martinez-Perez, C.; Mohr, W.; Loscher, C. R.; Dekaezemacker, J.; Littmann, S.; Yilmaz, P.; Lehnen,
471 N.; Fuchs, B. M.; Lavik, G.; Schmitz, R. A.; LaRoche, J.; Kuypers, M. M. *Nat Microbiol* **2016**, *1*, 16163
- 472 (19) Wang, Y.; Huang, W. E.; Cui, L.; Wagner, M. *Curr. Opin. Biotechnol.* **2016**, *41*, 34-42.
- 473 (20) Huang, W. E.; Griffiths, R. I.; Thompson, I. P.; Bailey, M. J.; Whiteley, A. S. *Anal. Chem.* **2004**, *76*,
474 4452-4458.
- 475 (21) Patzold, R.; Keuntje, M.; Theophile, K.; Muller, J.; Mielcarek, E.; Ngezahayo, A.; Ahlften, A. A. V. *J.*
476 *Microbiol. Methods* **2008**, *72*, 241-248.
- 477 (22) Millo, D.; Harnisch, F.; Patil, S. A.; Ly, H. K.; Schroder, U.; Hildebrandt, P. *Angew. Chem. Int. Edit.*
478 **2011**, *50*, 2625-2627.
- 479 (23) Virdis, B.; Harnisch, F.; Batstone, D. J.; Rabaey, K.; Donose, B. C. *Energ Environ Sci* **2012**, *5*,
480 7017-7024.
- 481 (24) Kubryk, P.; Kolschbach, J. S.; Marozava, S.; Lueders, T.; Meckenstock, R. U.; Niessner, R.; Ivleva, N.
482 *P. Anal. Chem.* **2015**, *87*, 6622-6630.
- 483 (25) N., V. K. B.; Kampe, B.; Röschab, P.; Popp, J. *Analyst* **2015**, *140*, 4584-4593.
- 484 (26) Li, M. Q.; Canniffe, D. P.; Jackson, P. J.; Davison, P. A.; FitzGerald, S.; Dickman, M. J.; Burgess, J. G.;
485 Hunter, C. N.; Huang, W. E. *ISME J.* **2012**, *6*, 875-885.
- 486 (27) Lutz, M. J. *Raman Spectrosc.* **1974**, *2*, 497-516.

- 487 (28) Berry, D.; Mader, E.; Lee, T. K.; Woebken, D.; Wang, Y.; Zhu, D.; Palatinszky, M.; Schintmeister, A.;
488 Schmid, M. C.; Hanson, B. T.; Shterzer, N.; Mizrahi, I.; Rauch, I.; Decker, T.; Bocklitz, T.; Popp, J.; Gibson,
489 C. M.; Fowler, P. W.; Huang, W. E.; Wagner, M. *Proc. Natl. Acad. Sci. U. S. A.* **2015**, *112*, E194-E203.
490 (29) Huang, W. E.; Stoecker, K.; Griffiths, R.; Newbold, L.; Daims, H.; Whiteley, A. S.; Wagner, M.
491 *Environ. Microbiol.* **2007**, *9*, 1878-1889.
492 (30) Muhamadali, H.; Chisanga, M.; Subaihi, A.; Goodacre, R. *Anal. Chem.* **2015**, *87*, 4578-4586.
493 (31) Cui, L.; Yang, K.; Zhou, G.; Huang, W. E.; Zhu, Y. G. *Anal. Chem.* **2017**, *89*, 5793-5800.
494 (32) Mariotti, A. *Nature* **1983**, *303*, 685-687.
495 (33) Burmolle, M.; Hansen, L. H.; Oregaard, G.; Sorensen, S. J. *Microb Ecol* **2003**, *45*, 226-236.
496 (34) Cui, L.; Butler, H. J.; Martin-Hirsch, P. L.; Martin, F. L. *Anal Methods-Uk* **2016**, *8*, 481-487.
497 (35) Cui, L.; Zhang, Y.-J.; Huang, W. E.; Zhang, B.-F. M., Francis L; Li, J.-Y.; Zhang, K.-S.; Zhu, Y.-G. *Anal.*
498 *Chem.* **2016**, *88*, 3164-3170.
499 (36) Zhang, B.; Cui, L.; Zhang, K. *Anal Bioanal Chem* **2016**, *408*, 3853-3865.
500 (37) Luo, T.; Ou-Yang, X. Q.; Yang, L. T.; Li, Y. R.; Song, X. P.; Zhang, G. M.; Gao, Y. J.; Duan, W. X.; An, Q.
501 *J. Basic Microbiol.* **2016**, *56*, 934-940.
502 (38) Feng, C.; Li, J.; Qin, D.; Chen, L.; Zhao, F.; Chen, S.; Hu, H.; Yu, C. P. *Plos One* **2014**, *9*, e113379.
503 (39) Streckas, T. C.; Spiro, T. G. *Biochim. Biophys. Acta* **1972**, *278*, 188-192.
504 (40) Xu, J.; Webb, I.; Poole, P.; Huang, W. E. *Anal. Chem.* **2017**, *89*, 6336-6340.
505 (41) Poole, R. K.; Hill, S. *Biosci. Rep.* **1997**, *17*, 303-317.
506 (42) Droghetti, E.; Oellerich, S.; Hildebrandt, P.; Smulevich, G. *Biophys. J.* **2006**, *91*, 3022-3031.
507 (43) Hu, S. Z.; Morris, I. K.; Singh, J. P.; Smith, K. M.; Spiro, T. G. *J. Am. Chem. Soc.* **1993**, *115*,
508 12446-12458.
509 (44) Jochum, T.; Fastnacht, A.; Trumbore, S. E.; Popp, J.; Frosch, T. *Anal. Chem.* **2017**, *89*, 1117-1122.
510 (45) Keiner, R.; Herrmann, M.; Kusel, K.; Popp, J.; Frosch, T. *Anal. Chim. Acta* **2015**, *864*, 39-47.
511 (46) Paul, E. A. *Soil Microbiology, Ecology and Biochemistry*; Academic Press: Boston, 2014.
512

513 **Supporting Information Available:** Experimental description of 16s rRNA and *nifH*
514 gene sequencing. Phylogenic trees. Deconvolution of Raman band and correlation of
515 band area ratio with ¹⁵N₂ percentage. Raman spectra of other types of N₂-fixing
516 bacteria and related bacteria.

517 **Author information**

518 Corresponding Author

519 *E-mail, ygzhu@rcees.ac.cn. Phone: 86-5926190997.

520 The authors declare no competing financial interest.

521

522 **Acknowledgements**

523 This work was supported by National Key Research and Development Program of
524 China (2017YFD0200201, 2017YFE0107300), the Strategic Priority Research
525 Program of Chinese Academy of Sciences (XDB15020302, XDB15020402), Natural
526 Science Foundation of China (21777154) and K.C.Wong Education Foundation.

527

528

529

530

531

532

533

534

535

536

537

538

539

540

541

542

543

544

545

546 **Figure legends**

547 **Figure 1.** Gel image of PCR product of *nifH* genes specific for N₂ fixation (a) and
548 single-cell resonance Raman spectra (b) from N₂-fixing bacteria isolated from soil
549 (red), model N₂-fixing bacteria (blue), non N₂-fixing *S. oneidensis* and *E. coli* (black).
550 'No template control' in gel image is the negative control without DNA template for
551 PCR.

552 **Figure 2.** (a) Single-cell resonance Raman spectra of *Azotobacter* sp. incubated with
553 ¹⁵N₂ of 99.36%, 49.68%, 25.02%, 10.22%, 0.36% relative to N₂ in air. (b) Spectral
554 region including exclusively 1114 cm⁻¹ (C-¹⁵N) and 1129 cm⁻¹ (C-¹⁴N) bands
555 extracted from a. (c) Correlation between incubation ¹⁵N₂ percentage versus
556 ¹⁵N-induced spectral changes in single cell based on PCA 1-D scores. Each point is a
557 measurement of a single cell, and around 25 cells were measured. (d) Quantification
558 of bulk ¹⁵N content in *Azobacter* sp. from the same incubation as in Raman as
559 detected by isotope ratio mass spectroscopy. ¹⁵N abundance in *E. coli* and *S.*
560 *oneidensis* incubated with 99.36% N₂ was also shown. (e) Correlation between ¹⁵N
561 content of *Azobacter* sp (from d) and PC1 scores (from c). Data points on the right of
562 c and d labeled as soil bacteria were from active N₂-fixing and non or weak N₂-fixing
563 soil bacteria.

564 **Figure 3.** (a) Photomicrograph of a mixed artificial community containing N₂-fixing
565 *Azotobacter* sp. incubated with ¹⁵N₂ in N-free medium and non-N₂-fixing *S.*
566 *oneidensis* grown in LB medium - two images showing the different shapes
567 (isospherical vs. rod-shaped) of these two bacteria are shown below. (b)

568 Corresponding Raman image from the same area as in a. (c) Typical Raman spectra
569 acquired from *Azotobacter* sp. and *S. oneidensis* in a and b. Bands at 1114 cm^{-1}
570 ($\text{C-}^{15}\text{N}$) and 1129 cm^{-1} ($\text{C-}^{14}\text{N}$), representing $^{15}\text{N}_2$ -fixing (red) and non- N_2 -fixing
571 bacteria (green), were employed to construct the Raman image.

572 **Figure 4.** Single-cell Raman spectra of diverse soil bacteria extracted from soil after
573 12-day incubation with $^{15}\text{N}_2$. Each spectrum represents a characteristic phenotype. i,
574 N_2 -fixing bacteria; ii, bacteria containing Cyt c but unable to fix N_2 ; iii and iv,
575 bacteria containing both Cyt c and carotenoid but unable to fix N_2 ; v, bacteria without
576 any pigment.

577 **Figure 5.** (a, b) Photomicrograph (left) and Raman images (right) of bacteria
578 extracted from soil microcosms incubated with $^{15}\text{N}_2$ for 12 days. (c) Resonance
579 Raman spectra of single cells from six N_2 -fixing bacteria (^{15}N -1, 2, 3, 4, 5, 6),
580 non- N_2 -fixing bacteria (^{14}N), and bacteria without Cyt c (no Cyt c) in a and b. Bands
581 at 1114 cm^{-1} ($\text{C-}^{15}\text{N}$) and 1129 cm^{-1} ($\text{C-}^{14}\text{N}$) were used to construct the Raman images
582 exhibiting N_2 -fixing bacteria as red, non- N_2 -fixing bacteria containing Cyt c as green,
583 and bacteria without Cyt c as black.

584

585

586

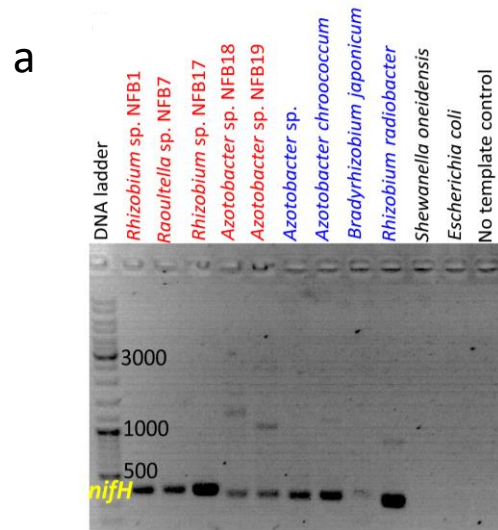
587

588

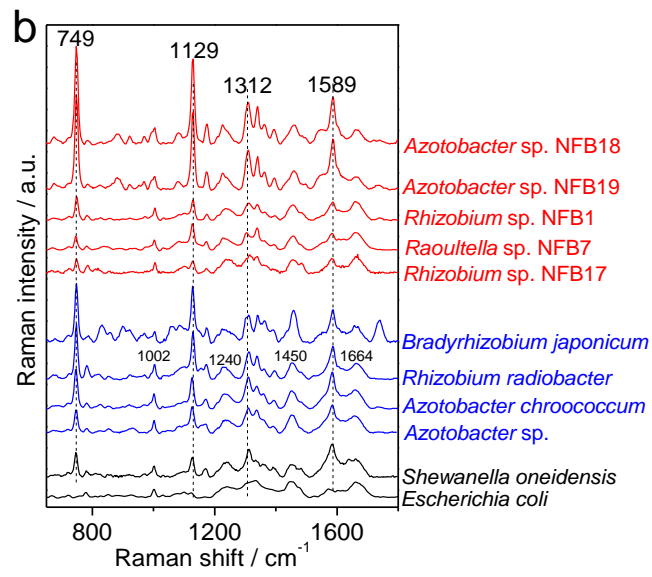
589

590

591



592



593

594

Figure 1

595

596

597

598

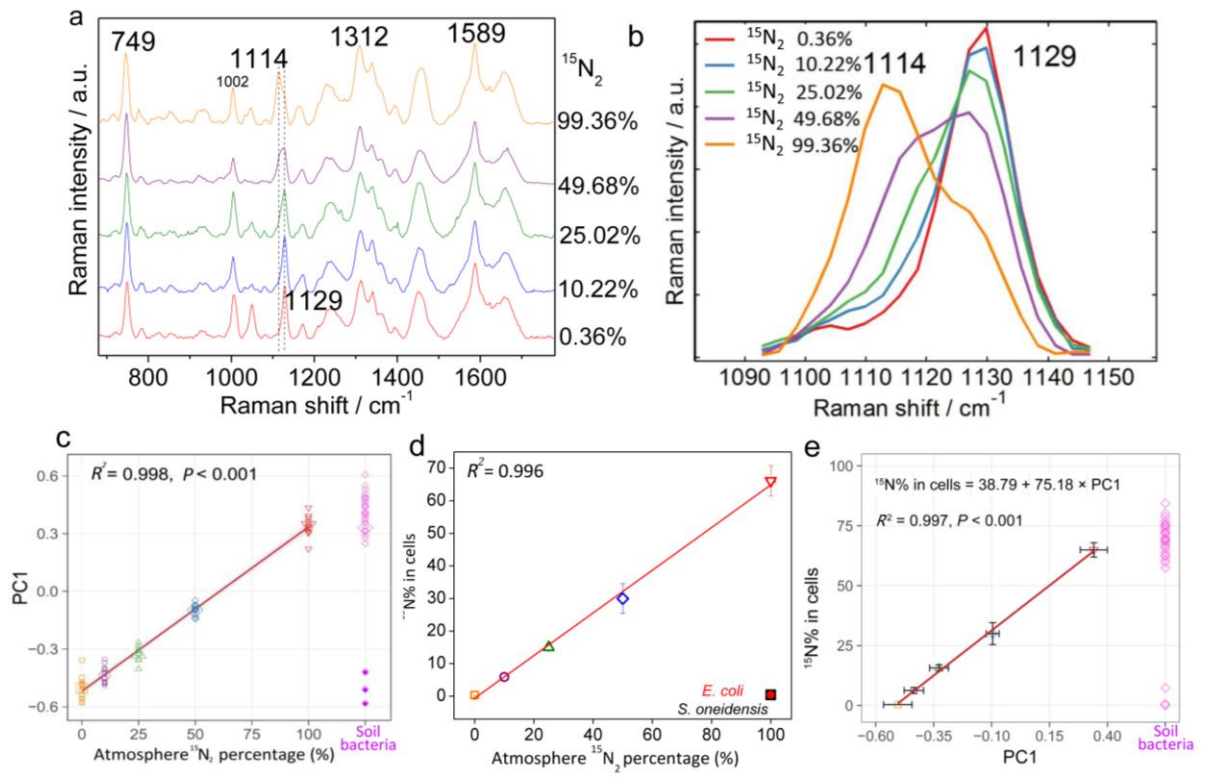


Figure 2

599

600

601

602

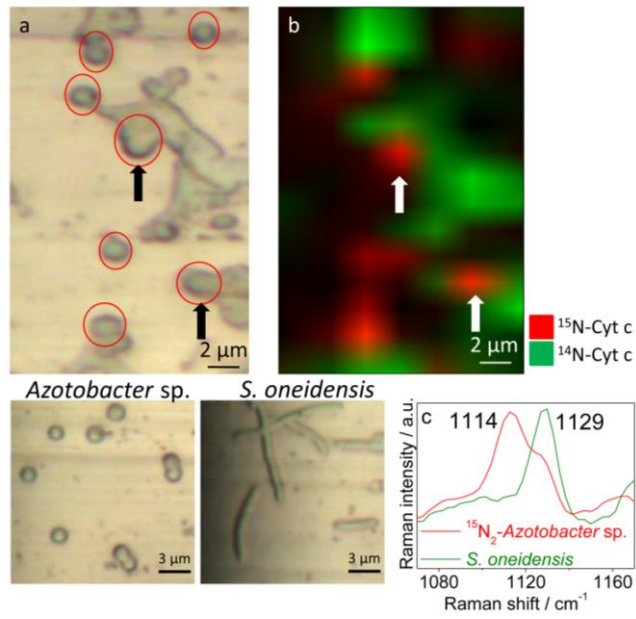
603

604

605

606

607



608

609

Figure 3

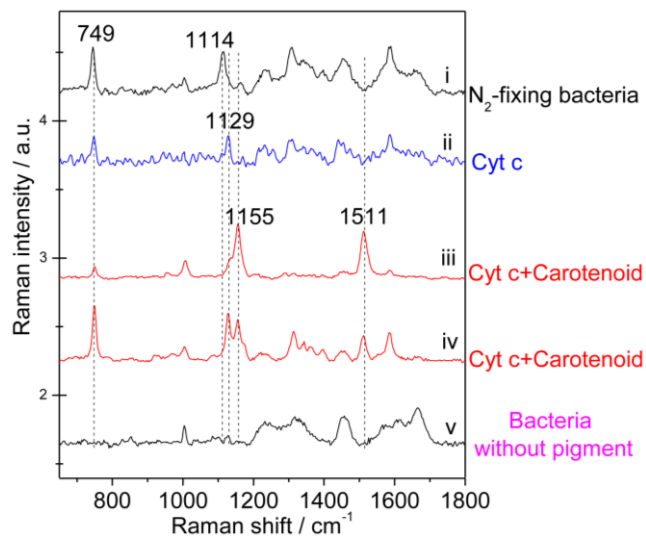
610

611

612

613

614



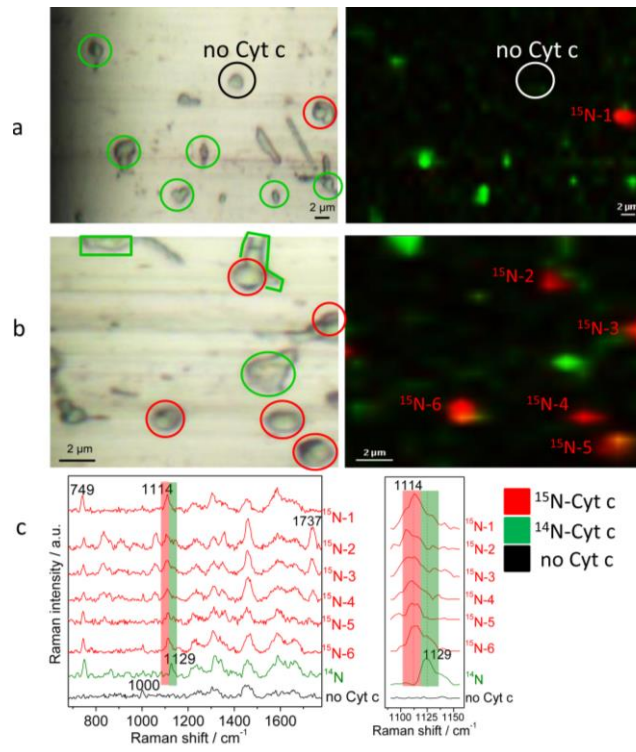
615

616

Figure 4

617

618



619

620

Figure 5